Half-metallic chromium dioxide (CrO_2) nanostructures and field-dependent magnetic domain evolution

Xiaojing Zou and Gang Xiao[a)]
Department of Physics, Brown University, Providence, Rhode Island 02912, USA

(Presented on 8 November 2007; received 12 September 2007; accepted 22 October 2007; published online 17 January 2008)

Both polycrystalline and epitaxial chromium dioxide structures in nanoscale have been fabricated using selective-area growth technique. Multiple grains were formed in the polycrystalline CrO_2 dots larger than 100 nm, however, below which only a single grain was allowed to exist. The lateral growth rate of epitaxial CrO_2 nanocrystals was found to be highly anisotropic, which is affected by both the orientation and the deposited thickness. Field-dependent magnetic force microscopy was used to study the domain structures of single crystal CrO_2 nanowires. The magnetization states were found to be closely related to the wire width. A stripelike domain structure with alternating magnetization parallel to the magnetic easy axis was observed within the CrO_2 nanowires aligned along the [010] directions, indicating the existence of a strong uniaxial magnetocrystalline anisotropy. © *2008 American Institute of Physics*. [DOI: 10.1063/1.2832315]

Ferromagnets with high spin polarization have been investigated intensively in the field of spintronics to realize spin-dependent devices with high performance such as tunneling magnetoresistance.[1] An important material category in this field, referred to as half metals, consists of materials that have 100% spin polarization at the Fermi level. The existence of such ferromagnets was predicted theoretically long time ago.[2,3] However, experimentally, chromium dioxide (CrO_2) is the only material that has been unambiguously determined to be half metallic.[4,5]

Studies on different properties of CrO_2 have been carried out in the past several years. However, most of the researches were done on bulk films or micron-sized structures. On the other hand, magnetic behaviors are closely related to the element size and dimensionality.[6] As the length scales approach the size of domain wall widths (nanometer scale), lateral confinement and interparticles exchange effects may dominate, rendering different properties from bulk materials. Thus, both for applications and for understanding the fundamental spin-related physics, the study of half-metallic CrO_2 nanostructures is of significance.

In this work, we report on the fabrication process of both polycrystalline and epitaxial CrO_2 nanostructures. The difference between them is discussed with emphasis on the anisotropic lateral growth rate of epitaxial nanodots. We have investigated the field-dependent domain structures of single crystal CrO_2 nanowires using magnetic force microscopy (MFM).

High quality chromium dioxide films can be grown using chemical vapor deposition (CVD) technique with chromium trioxide as a precursor.[7] The crystal properties of CrO_2 films made this way are greatly affected by the substrate used. Epitaxial (100)-CrO_2 structures were deposited pseudo morphically on single crystal (100)-TiO_2 substrates. We also grew polycrystalline CrO_2 structures, based on a seed layer of polycrystalline TiO_2 film, which was made by oxidizing at 800 °C the Ti film (~100 nm) sputtered on SiO_2-covered silicon wafer.

Since chromium dioxide is not a thermodynamically stable phase at atmospheric pressure and room temperature, it inevitably decomposes and forms a native oxide Cr_2O_3 layer on the surface. Prior to this work, various methods have been attempted to pattern CrO_2 small structures such as reactive ion etching (RIE),[8] wet etching, argon-ion milling,[9] and focused ion beam milling.[10] All these methods applied etching to deposited chromium dioxide thin films, which increased the transformation from CrO_2 to Cr_2O_3, resulting in degradation of the quality of CrO_2. An alternative approach to make chromium dioxide structures is the selective-area growth technique.[11] It utilizes the fact that during the CVD process, CrO_2 grows readily on the surface of TiO_2 but not on amorphous SiO_2. This way avoids the postdeposition etching and subsequent reduction of CrO_2. In this work, we have extended the selective-area growth technique and obtained CrO_2 nanostructures down to sub-100-nm scale.

The fabrication process is described as follows. First, a layer of SiO_2 (~100 nm) was deposited onto the TiO_2 substrate by radio frequency magnetron sputtering of a Si target in a mixture of argon and oxygen. Then, a layer of positive polymethylmethacrylate (PMMA) with molecular weight of 950 kD was spin coated onto the sample. After a bake at 185 °C for 30 min, the sample was covered with a very thin layer of Cr (~5 nm) by electron beam evaporation, which served as a charge dissipation layer during the subsequent electron beam lithography. The Cr layer was first removed in chemical etchant solution, and then the sample was developed for 60–65 s in a 1:3 solution of methyl isobutyl ketone: isopropyl alcohol (IPA) followed by rinsing in IPA. The developed PMMA was used as the etching mask for the RIE of the underlying SiO_2 layer in the CHF_3 atmosphere. Finally, the sample was carefully cleaned in acetone, IPA, and de-

[a)]Electronic mail: gang_xiao@brown.edu.

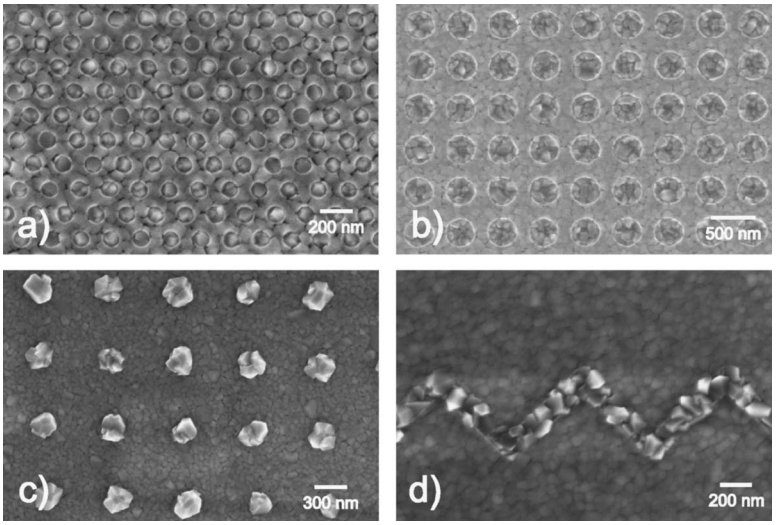

FIG. 1. SEM images of polycrystalline CrO_2 nanostructures: (a) 100 nm sized dots array, (b) 250 nm sized dots array, (c) overgrown CrO_2 from 150 nm sized holes, and (d) a zigzag-shaped nanowire with 150 nm in width. The small patterns other than the CrO_2 structures are the polycrystalline TiO_2 grains below the amorphous SiO_2.

ionized water before loading into furnace to deposit CrO_2 using CVD.

The scanning electron microscopy (SEM) images of polycrystalline CrO_2 nanodot arrays are shown in Figs. 1(a) and 1(b). We can see that multiple grains are formed in the dots with diameter $d=250$ nm. However, when d is reduced to about 100 nm, each dot contains only one single grain. This can be understood by considering that, when the size of the holes on the SiO_2 template is smaller than the mean grain diameter of the TiO_2 substrate ($\sim$100 nm), there is only one TiO_2 grain below each hole to support the growth of CrO_2. Upon increasing the thickness, the deposited CrO_2 reaches the top of the mask and then overgrows both vertically and laterally. Figure 1(c) displays the overgrown CrO_2 from 150 nm sized holes. As can be seen, the borders of the holes are completely covered by the CrO_2 above the SiO_2 mask. The SEM image of a 150 nm wide zigzag wire is shown in Fig. 1(d). The clear grain facets and borders reflect that every grain was grown naturally without any postdeposition damage.

Figure 2(a) displays the SEM image of 100 nm sized epitaxial CrO_2 nanodots. As can be observed, all the dots are distinct and aligned in the same crystal direction. Figures 2(b)–2(d) show the morphology of the CrO_2 nanodots with different deposited thicknesses t. All the dots grew naturally into a rectangular shape, which implies that the lateral (in-plane) growth rate was anisotropic during the CVD process. Otherwise, the dots would form a round shape instead of a rectangular one, since the antidot patterns defined on the SiO_2 template were circular. Furthermore, we can see that the aspect ratio of the rectangle is not a constant, and changes with the CrO_2 thickness. Hence, the mean lateral growth rate V is affected by both the direction, represented by angle θ in Fig. 2(f), and the thickness t of the deposited CrO_2.

The CrO_2 nanocrystal growth process can be physically described as follows. At the beginning of the deposition, CrO_2 first covered the TiO_2 at the bottom of the holes, but not the adjoining SiO_2 due to the selective-area growth. Then beyond a certain thickness, the deposited CrO_2 deformed with a preferential lateral growth direction along the c axis, as evidenced in Fig. 2(b). This means that when t was small, $V(\theta,t)$ was maximum for $\theta_m \approx 0°$. It can be attributed to the fact that there is a large lattice mismatch between TiO_2 and CrO_2, of -3.79% along the b axis ([010] direction) and only 1.48% along the c axis ([001] direction). The chemical vapor deposition favors the growth along the [001] direction for higher lattice match in order to reduce the internal strain energy. When t increased, CrO_2 starts to overgrow laterally over the amorphous SiO_2 mask. We can see in Fig. 2(c) that in the meanwhile a rectangular shape with long side parallel to the c axis was formed for every dot, indicating the maximum $V(\theta,t)$ was achieved at an angle θ_m between 0° and 45°, more specifically, the diagonal direction of the rect-

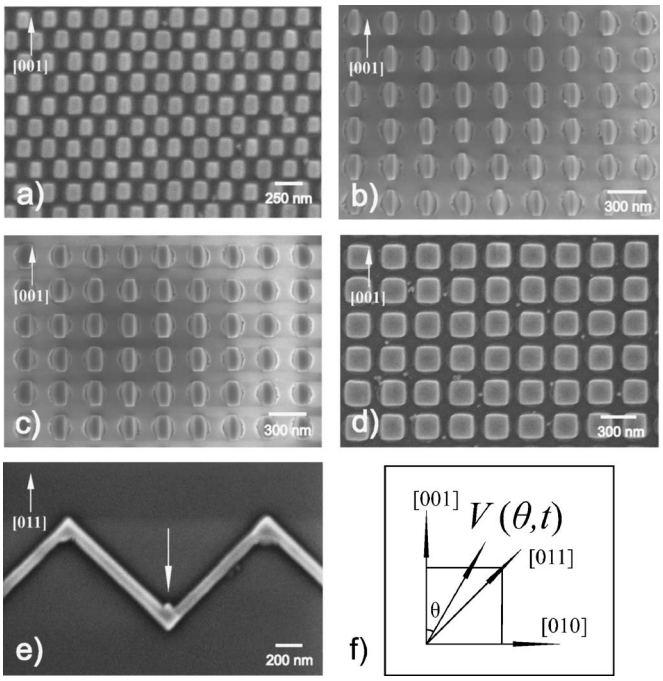

FIG. 2. SEM images of single crystal CrO_2 nanostructures grown on (100)-TiO_2 substrate: (a) 100 nm sized dot array, 250 nm sized dot array with different thicknesses (b) $t=100$ nm, (c) $t=160$ nm, and (d) $t=250$ nm; (e) a 100 nm wide zigzag wire with overgrown CrO_2 along the [011] direction, and (f) schematic diagram for the mean lateral growth rate V dependent on the orientation, represented by angle θ.

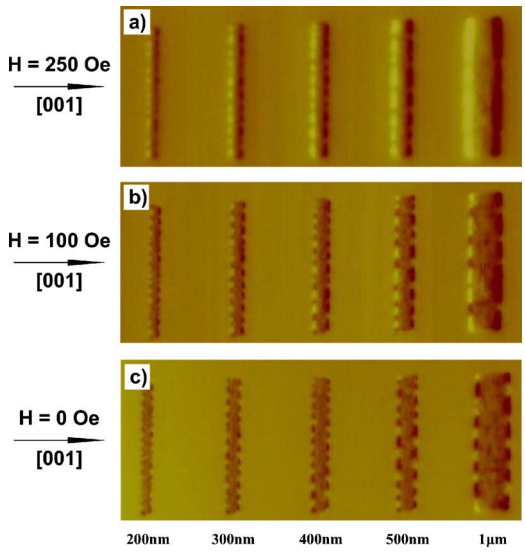

FIG. 3. (Color online) Magnetic field dependent MFM images of epitaxial CrO_2 nanowires aligned along the [010] direction with different linewidths. The field is applied in the [001] direction with value H: (a) 250 Oe, (b) 100 Oe and (c) 0 Oe.

angle. Upon further increasing the amount of overgrown CrO_2, the aspect ratio of the rectangular dots gradually became smaller and stabilized to 1. Our result reveals that when t is large ($\geqslant$250 nm), $V(\theta,t)$ is maximum for $\theta_m = 45°$ ([011] direction) giving every dot a square shape. The preferred lateral growth along the [011] direction can also be observed in epitaxial CrO_2 zigzag nanowire shown in Fig. 2(e). At this point, the detailed kinetic process for the transformation from a high-aspect-ratio rectangle to a square is unknown. However, we believe that the anisotropic surface binding energy drives this CrO_2 nanocrystal growth. Other factors, such as the internal strain due to the lattice mismatch, may also play an important role.

We also investigated the magnetic switching behavior of the epitaxial chromium dioxide nanowires using field-dependent MFM. The sample was first saturated along the magnetic easy axis ([001] direction) and then imaged with a field H applied in the same direction. Figure 3 displays the MFM images of CrO_2 wires of various linewidths w aligned along the [010] axis under three different external fields. A single domain structure with magnetization along the applied field direction was observed in Fig. 3(a) for the epitaxial wire with $w=1$ μm. Upon decreasing the linewidth, multidomain structures were formed with a small number of domains having opposite polarities. This result can be explained by considering the demagnetizing field H_d, which was found to be roughly proportional to the inverse of linewidth $1/w$.[12] When w decreased from 1 μm to 200 nm, the internal field, $H_{\text{int}} = H_{250\ \text{Oe}} - H_d$, dropped significantly and thus was energetically unfavorable to maintain a single domain structure. In Fig. 3(b) where the external field H was reduced to 100 Oe, the nucleation of antiparallel domains can be clearly observed as the number of domains with the magnetization reverse to the field direction increased. When the magnetic field was further reduced to zero, the MFM image reflects the remanent magnetization state, which is displayed in Fig. 3(c). A stipelike domain structure, with magnetization parallel or antiparallel to the magnetic easy axis, was observed. It should be noted that the remanent state of the epitaxial CrO_2 nanowires are determined mainly by both the shape and magnetocrystalline anisotropy. The former favors an alignment of the magnetic moment parallel to the wire axis, while the latter prefers the magnetic easy axis direction. In our case, the wire axis is perpendicular to the magnetic easy axis, which means that these two effects are in competition with each other. The existence of stripelike domain configuration even for the wire with $w=200$ nm indicates that the magnetocrystalline anisotropy in epitaxial CrO_2 is very strong, which makes the shape induced effect almost negligible. Upon further increasing the field in the reverse direction, domains start to annihilate and a similar reversal process has been observed (not shown here).

In summary, we present a new method to fabricate both polycrystalline and single crystal chromium dioxide nanostructures. The use of the selective-area growth technique prevents the damage caused by postdeposition etching and allows us to study the nanocrystal growth process. The epitaxial lateral overgrowth rate was found to be maximum at the [011] directions of (100)-TiO_2 substrate. We have also investigated the magnetic reversal process of epitaxial CrO_2 nanowires. Due to the strong magnetocrystalline anisotropy, stripe-domain structures were observed for wires with axes perpendicular to the magnetic easy axis direction.

This work was supported in part by the NSF under Grant No. DMR-0605966. We also gratefully acknowledge partial support from JHU MRSEC (No. NSF DMR-0520491).

[1] G. A. Prinz, Science **282**, 1660 (1998).
[2] C. M. Fang, G. A. de Wijs, and R. A. de Groot, J. Appl. Phys. **91**, 8340 (2002).
[3] S. P. Lewis, P. B. Allen, and T. Sasaki, Phys. Rev. B **55**, 10253 (1997).
[4] Y. Ji, G. J. Strijkers, F. Y. Yang, C. L. Chien, J. M. Byers, A. Anguelouch, G. Xiao, and A. Gupta, Phys. Rev. Lett. **86**, 5585 (2001).
[5] R. J. Soulen, Jr., J. M. Byers, M. S. Osofsky, B. Nadgorny, T. Ambrose, S. F. Cheng, P. R. Broussard, C. T. Tanaka, J. Nowak, J. S. Moodera, A. Barry, and J. M. D. Coey, Science **282**, 85 (1998).
[6] J. F. Bobo, L. Gabillet, and M. Bibes, J. Phys.: Condens. Matter **16**, S471 (2004).
[7] X. W. Li, A. Gupta, and G. Xiao, Appl. Phys. Lett. **75**, 713 (1999).
[8] Q. Zhang, Y. Li, A. V. Nurmikko, G. X. Miao, G. Xiao, and A. Gupta, J. Appl. Phys. **96**, 7527 (2004).
[9] C. Konig, M. Fonin, M. Laufenberg, A. Biehler, W. Buhrer, M. Klaui, U. Rudiger, and G. Guntherodt, Phys. Rev. B **75**, 144428 (2007).
[10] L. Yuan, Y. Ovchenkov, A. Sokolov, C.-S. Yang, B. Doubin, and S. H. Liou, J. Appl. Phys. **93**, 6850 (2003).
[11] A. Gupta, X. W. Li, S. Guha, and G. Xiao, Appl. Phys. Lett. **75**, 2996 (1999).
[12] B. Pant, J. Appl. Phys. **67**, 414 (1989).